



OPEN ACCESS

EDITED BY

Michael Ojovan,
The University of Sheffield, United Kingdom

REVIEWED BY

John L. Provis,
Paul Scherrer Institut (PSI), Switzerland
Nailia Rakhimova,
Kazan State University of Architecture and
Engineering, Russia

*CORRESPONDENCE

Ayelén Manzini,
✉ ayelenmanzini@cnea.gov.ar

RECEIVED 03 November 2025

REVISED 10 December 2025

ACCEPTED 15 December 2025

PUBLISHED 11 February 2026

CITATION

Talavera Ramos W, Tellería Narváez A,
Dos Santos L, Arcone D and Manzini A (2026)
First evaluation of geopolymer encapsulation of
simulated alkaline aluminum-rich liquid waste
from Mo-99 production.
Front. Nucl. Eng. 4:1738676.
doi: 10.3389/fnuen.2025.1738676

COPYRIGHT

© 2026 Talavera Ramos, Tellería Narváez, Dos Santos, Arcone and Manzini. This is an open-access article distributed under the terms of the [Creative Commons Attribution License \(CC BY\)](https://creativecommons.org/licenses/by/4.0/). The use, distribution or reproduction in other forums is permitted, provided the original author(s) and the copyright owner(s) are credited and that the original publication in this journal is cited, in accordance with accepted academic practice. No use, distribution or reproduction is permitted which does not comply with these terms.

First evaluation of geopolymer encapsulation of simulated alkaline aluminum-rich liquid waste from Mo-99 production

Whitney Talavera Ramos¹, Adrián Tellería Narváez¹,
Lucas Dos Santos¹, Daniel Arcone² and Ayelén Manzini^{1*}

¹División Predisposición, Departamento de Investigación y Tecnología Aplicadas (DITA), Programa Nacional de Gestión de Residuos Radiactivos (PNGRR), Comisión Nacional de Energía Atómica (CNEA), Buenos Aires, Argentina, ²Departamento Materiales Avanzados, Gerencia Materiales, Comisión Nacional de Energía Atómica, Buenos Aires, Argentina

This study investigates the synthesis and characterization of metakaolin-based geopolymers for the immobilization of simulated aluminum-containing radioactive liquid waste. Two kaolin precursors with different Si/Al ratios and purities were calcined between 700 °C and 900 °C. Geopolymers were prepared using a sodium silicate–NaOH activating solution (10 M NaOH) with and without sand, and cured at 60 °C. The effects of curing time and simulated liquid waste incorporation (10–40 wt%) on mechanical strength and microstructural development were evaluated through compressive strength tests, XRD, and SEM analyses. The results showed that curing time influenced strength development. Incorporation of simulated liquid waste generally reduced compressive strength, probably due to increased porosity and decreased metakaolin (MK) dissolution; however acceptable performance was achieved at a 20 wt% addition for MKSR-based geopolymers. XRD analyses confirmed the formation of an amorphous band between 25° and 35° typical of geopolymer structures. In contrast, MKS-based geopolymers exhibited lower mechanical strength and incomplete gel formation under the tested conditions. These findings demonstrate the potential of local precursor MKSR metakaolin-based geopolymers as promising matrices for the immobilization of aluminum-bearing radioactive liquid waste.

KEYWORDS

alkaline aluminum liquids, geopolymer, immobilization, Mo-99 production, predisposal management, radioactive waste

1 Introduction

Radioactive waste, generated from chemical sludges, fission products, spent fuel, and reactor decommissioning, poses long-term environmental risks. It is classified by activity level into low (LLW), intermediate (ILW), and high-level (HLW) waste, each requiring specific disposal methods such as landfills, shallow disposal, or deep geological repositories with multi-barrier protection systems (Internationale Atomenergie-Organisation, 2003; International Atomic Energy Agency, 2013; Zheng et al., 2020). Immobilization techniques, like solidification and encapsulation, aim to reduce radionuclide migration. Materials like Portland Cement (PC), bitumen, glass, and steel are commonly used, though challenges remain regarding durability and corrosion. Recently, geopolymers have gained attention as a promising alternative to PC for radioactive waste immobilization (Garces et al., 2022).

The geopolymers consist of a three-dimensional network of silicate and aluminate tetrahedra linked by shared oxygen atoms, resulting in a highly crosslinked and durable structure (Zhang et al., 2016). Their general chemical formula can be expressed as $Mn[-(\text{SiO}_2)_z\text{AlO}_2]_n \cdot w\text{H}_2\text{O}$, where M represents an alkali cation (Na^+ , K^+ , or Cs^+), n is the degree of polymerization, z the Si/Al ratio, and w the water content (Glukhovskiy, 1959).

The geopolymerization mechanism generally involves the dissolution of aluminosilicate sources in an alkaline medium, followed by condensation and polycondensation reactions leading to the formation of a rigid amorphous network (Phair and Van Deventer, 2002). The properties of the resulting materials depend strongly on several factors, including the type of precursor, the nature and concentration of the alkaline activator, the Si/Al ratio, curing conditions, and water content (Stevenson et al., 2005; Barbosa et al., 2000; Geddes et al., 2024; Duxson et al., 2005; Duxson et al., 2007; Wang et al., 2018; Tian et al., 2019).

Geopolymers have attracted significant attention due to their excellent mechanical strength, chemical stability, resistance to heat and radiation. These properties make them promising candidates for nuclear waste immobilization, where long-term containment and resistance to leaching are critical (Khalil and Merz, 1994; Perera et al., 2007). Compared with Portland cement, geopolymers exhibit superior durability under extreme conditions, including high temperature, radiation exposure, and freeze–thaw cycles (Davidovits, 2020; Zhang et al., 2014; Li et al., 2013).

Recent studies have explored geopolymers as matrices for immobilizing both cationic and anionic radionuclides. While their negatively charged framework facilitates the incorporation of cations such as Cs^+ and Sr^{2+} through ion exchange and physical encapsulation, immobilization of anionic species (e.g., SeO_3^{2-} , SeO_4^{2-} , MoO_4^{2-}) remains challenging due to electrostatic repulsion (Arbel-Haddad et al., 2022; Jang et al., 2016; Munthali et al., 2015; El Alouani et al., 2021). Understanding how compositional and processing parameters influence the interaction between geopolymers and radionuclides is therefore essential to optimize their performance as solidification and stabilization materials for radioactive waste management (Pao and Chin, 2022).

This work presents a preliminary experimental approach to evaluate the incorporation of simulated alkaline liquid waste from the Mo-99 production process in Argentina into geopolymeric matrices. One of the waste streams generated in this process consists of aluminum-rich liquid effluents, which are currently stored in appropriate 200-L drums. Although some Portland-cement-based matrices have been evaluated for the immobilization of these simulated waste streams, their high aluminum content interferes with cement setting, ultimately affecting the mechanical properties of the final specimens (Marabini, 2023). Given that geopolymers are known to exhibit higher compressive strength, improved leaching performance, and reduced volumetric expansion, direct immobilization in this matrix was explored, taking advantage of the waste's high aluminum content and alkalinity as part of the reactants. In this first phase of the study, the alkaline aluminum-rich simulated waste (nonradioactive surrogates) loading will be assessed by varying the mass ratios between the geopolymer matrix and the simulated solution. The aim is to determine the impact of waste

incorporation on the geopolymer structure through compressive strength testing and complementary characterization techniques.

2 Materials and methods

2.1 Reactants

The kaolin used was from Sigma-Aldrich and Sur del Río (Argentina local provider). All of them were thermally treated for conversion to metakaolin using the following procedures: calcination to 700, 800 °C and 900 °C, using heating rate of 10 °C/min, and isotherm heating time at final temperature of 1 h. Before and after heating, reactants were characterized with XRD (Panalytical Empyrean). For the silicon source waterglass [$\text{Na}_2\text{O}_x(\text{SiO}_2)$, where x is approximately equal to 2.5] (Mapal and Sigma-Aldrich) was used as received. The NaOH 10 M solution was prepared from NaOH pellets (Sigma-Aldrich) and pure water type II.

2.2 Sample preparation

The geopolymer monoliths were prepared with the ratios shown in Table 1. These values are based on the recommendations of the 2021 PREDIS workshop (Tri et al., 2021). The pastes were prepared using a VELS Scientifica Stirrer DLS mixer at 800 rpm for 15 min. The mixtures were then poured into 30-mm-diameter and 47 mm height tubes, gently tapped to remove trapped air bubbles, and subjected to thermal curing under different periods of time. After demolding, samples were polished to obtain parallel surfaces.

The curing process was as follows: at 60 °C for periods of 4 h, 1 day, 2 days, 3 days, 4 days, 5 days, 6 days, 7 days and 8 days. After the curing period, the samples were demolded and left under ambient temperature (25 °C) and humidity (50% ± 5%) until testing.

To evaluate the geopolymers as immobilization matrices, aluminum-containing simulated waste solutions were mixed at 10, 20, 30, and 40 wt% with the synthesized geopolymers (at 90, 80, 70, and 60 wt%, respectively). The simulated solutions contain 9 wt% NaOH and 1.6 wt% aluminum. The remaining elemental composition is confidential.

Samples are identified after the kaolin brand name, SR for Sur del Río and S for Sigma-Aldrich, followed by a number which determines the percentage of simulated liquid waste added (e.g. GRSR-20S stands for geopolymer from Sur del Río metakaolin with 20% Al simulated waste and the final S stands for sand added in the formulation).

2.3 Compressive strength measurements

All samples were subjected to fracture tests using a INSTRON 8802 Servohydraulic Fatigue Testing instruments, at an axial displacement speed of 0.9 mm/min. Also, a ball-and-socket joint was used to counterbalance the lack of parallelism between the top and the bottom of the monoliths, assuring the compressive force to be evenly distributed across the section of the monolith's surface. This enhanced the reproducibility of the results despite some sample

TABLE 1 Formulations for each batch of geopolymers (mass%), from kaolin Sur del Río and kaolin Sigma-Aldrich.

	Sur del Río (SR)		Sigma-Aldrich (S)	
	Without aggregate	With aggregate	Without aggregate	With aggregate
Na ₂ O.xSiO ₂	51	36	41	30
NaOH [10 M]	5	4	4	3
MK	44	32	36	26
Water	-	-	19	18
Sand	-	28	-	23

TABLE 2 Elemental composition (mass%) of kaolin samples.

Element	SiO ₂	Al ₂ O ₃	Na ₂ O	CaO	Fe ₂ O ₃	SO ₃	K ₂ O	TiO ₂	MgO	P ₂ O ₅	Others	SiO ₂ /Al ₂ O ₃
Kaolin SR	57.0	28.5	0.091	0.181	0.957	0.085	0.691	0.366	0.166	0.014	11.9	3.39
Kaolin S	50.5	39.3	0.069	0.058	0.92	0.10	0.15	1.59	-	0.071	7.2	2.18

inhomogeneity and porosity. All measurements were performed in triplicate.

2.4 Characterization

X ray diffraction (XRD) measurements were undertaken on a Panalytical Empyrean diffractometer using Cu K α (1.5406 Å) radiation (40 kV, 40 mA) and a PIXcel3D detector. These measurements employed on the incident beam side a Soller slit of 0.04 radian, a programmable divergence slit of 1/2°, a 10 mm beam mask and a fixed anti scatter slit of 1°, while on the diffracted beam side a PM7.7 anti-scatter slit and a monochromator with included Soller were used. Samples were grinded and mounted for Bragg- Brentano configuration with a scanning rate of 3.76° per min from 5° to 70° of 2 θ , and 0.026° steps. Phases determination was analyzed with High Score software.

Scanning electron microscope (SEM) images were taken on a FEI Inspect F50 operating at 15 kV using a Backscattered Electron Detector. EDAX was performed by collecting data for 10 min.

TGA was used to determine temperature range for metakaolin conversion. The configuration used was a heating rate of 10 °C/min in air up to 1,000 °C.

WDXRF measurements were done with a Bruker S8 Tiger equipment. Samples were prepared using H₃BO₃ to form 40 mm pellets. The instrument uses an X-ray tube of rhodium operated at 40 kV and 10 mA with a Bragg-Brentano configuration. Measurements were acquired with the Spectra Plus software using the Quant-Express calibration, while samples employed 34 mm masks.

3 Results and discussion

3.1 Characterization of raw and calcined kaolin samples

Results of chemical composition of the kaolin samples obtained by XRF are given in Table 2. It appears that kaolin SR material has a

higher proportion of SiO₂ than kaolin S, probably due to the presence of quartz. The SiO₂/Al₂O₃ mole ratios of SR and S materials are 3.39 and 2.18 respectively, implying that kaolin SR has lower kaolinite content than that of kaolin S.

Figure 1 compares the XRD patterns of the kaolin S (Figure 1a) and SR (Figure 1b) samples calcined at 700, 800, and 900 °C for 1 h under a heating rate of 10 °C/min. The calcination temperature was selected starting from 700 °C based on the TGA analysis (not shown here), which revealed a significant mass loss likely associated with the thermal dehydroxylation of kaolinite (Elimbi et al., 2011) occurring between 450 °C and 650 °C.

A broad band between 18° and 25° can be observed in the calcined kaolin S samples (b, c, and d in Figure 1a), corresponding to the amorphous structure of metakaolin (Wang et al., 2005), along with quartz peaks of very low intensity. Similar results were obtained for the samples calcined at all three evaluated temperatures, suggesting that metakaolin suitable for geopolymer synthesis can be obtained at temperatures as low as 700 °C.

On the other hand, for the SR kaolin samples (b, c, and d in Figure 1b), the XRD patterns show the formation of a slight semi-amorphous metakaolin band between 18° and 25° after calcination, accompanied by the disappearance of all the intense kaolinite peaks present in the raw kaolin, and the persistence of a few residual quartz peaks. Again, no significant differences were observed among the diffractograms of samples treated at different temperatures.

Based on these results, all SR and S kaolin samples were calcined at 800 °C for the synthesis of the geopolymers.

3.2 Influence of curing time

The curing time is a key parameter influencing the mechanical strength of materials (Palomo et al., 1999; Rovnanik, 2010). In this context, the influence of curing time on the compressive strength of geopolymer samples synthesized with and without sand was studied at the age of 4h, 1, 2, 3, 4, 5, 6, 7, and 8 days after mixing and at a

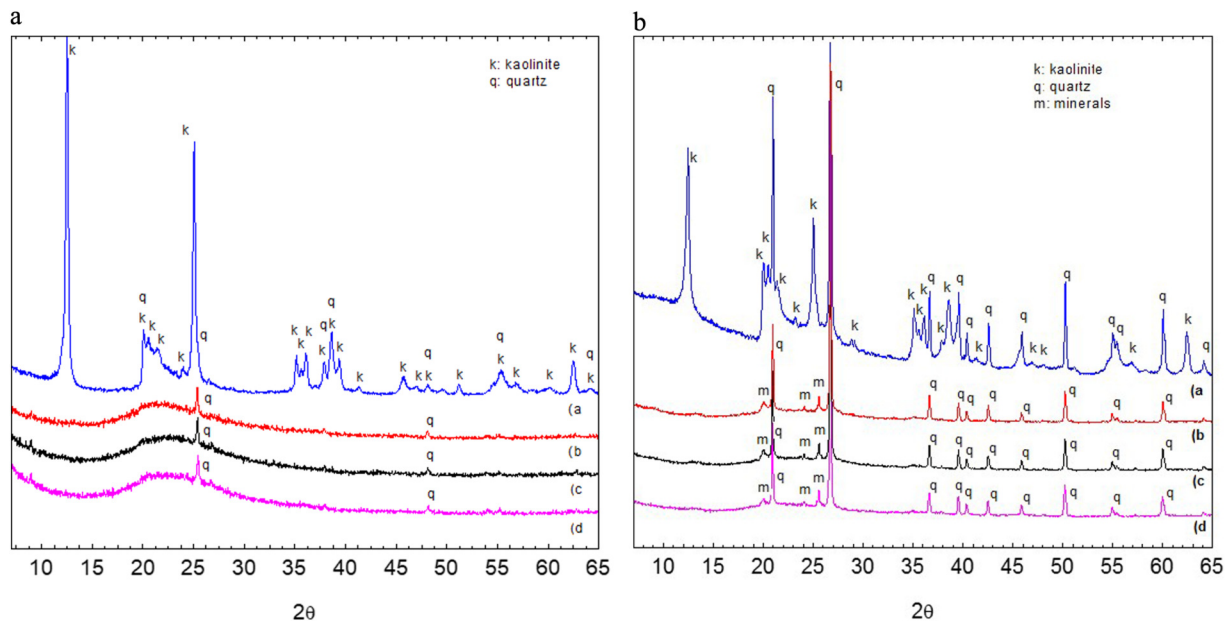


FIGURE 1 X-rays diffractograms of the SR kaolin (a) and S kaolin (b) calcined at different temperatures. In (a): (a) KS, (b) MKS-700, (c) MKS-800, (d) MKS-900. In (b): (a) KSR, (b) MKSR-700, (c) MKSR-800, and (d) MKSR-900.

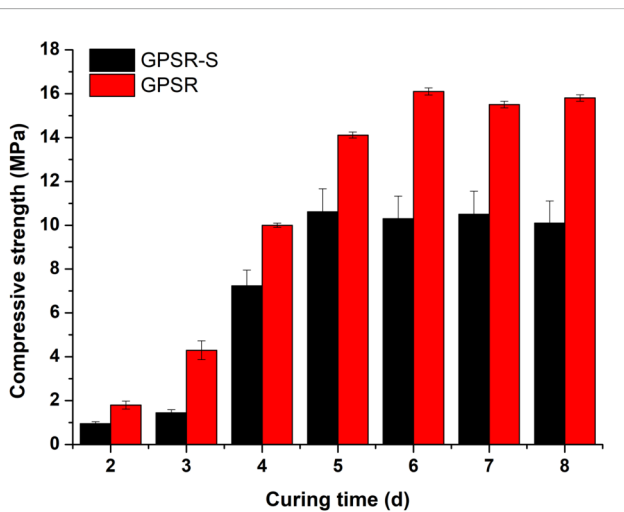


FIGURE 2 Influence of the curing time on the compressive strength to GPSR with (GPSR-S) and without (GPSR) sand samples.

temperature of 60 °C. It has been reported that, at early ages, strength increases with temperature due to an increase in the degree of geopolymerization and, consequently, in the amount of reaction products (Rovnaník, 2010). Therefore, a curing temperature of 60 °C was chosen as an intermediate value to facilitate geopolymerization over short curing periods (up to 8 days), as this temperature has been reported by other researchers to be optimal. The compressive strength of samples cured at 60 °C was higher than that of samples treated at 40 °C and very similar to those cured at 80 °C (Rovnaník, 2010; García-Mejía and de Lourdes Chávez-García, 2016).

The geopolymers were prepared from kaolin SR calcined at 800 °C for 1 h, with a heating rate of 10 °C/min, using a liquid sodium silicate solution in 10 M NaOH as the activating medium. The samples were designated as GPSR-S or GPSR, where S represents sand. The results are shown in Figure 2. It can be observed that the compressive strength of the samples with and without sand increases with the curing time, being higher in the case of the samples containing sand. This behavior is attributed to a probable porosity reduction and to a reinforcement effect of the sand particles in the geopolymer matrix (Kuenzel et al., 2014). The samples cured for 4 h and 1 day did not set; therefore, compressive strength testing could not be performed.

In the micrographs obtained by SEM (Figure 3), it can be observed that the sample cured for 2 days without sand (GPSR-2, see Supplementary Figures SI, SI1) exhibits a heterogeneous surface morphology, closely resembling that of the metakaolin precursor (MKSR, Figure 3a), with solid flake-like metakaolin particles. After 7 days, the surface of the sample cured without sand (GPSR-7, Figure 3b) appears more homogeneous, with smoother and more compact areas, suggesting that a higher degree of geopolymerization occurs within this curing period compared to the samples cured for only 2 days. Elemental mapping performed by EDX (not shown here) revealed that the elemental distribution, mainly of Al, Si, and O, was uniform across the surface of the samples, suggesting a homogeneous geopolymerization process. The samples cured for 8 days exhibited similar morphological characteristics; therefore, their micrographs are not shown. Similarly, the micrographs of sand-containing samples were comparable to those without sand and are therefore not presented.

Since the XRD diffractograms of all samples did not reveal significant differences, and thus, the corresponding patterns are not shown.

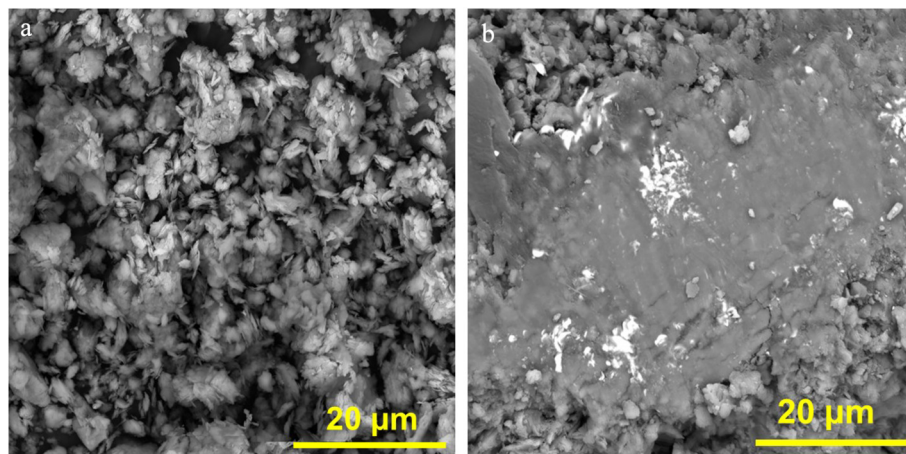


FIGURE 3
Micrographs of samples: (a) MKSR, (b) GPSR-7.

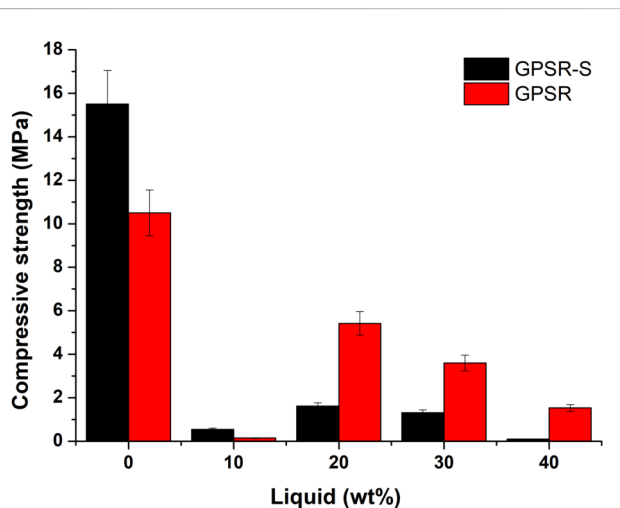


FIGURE 4
Compressive strength versus mass percent of simulated aluminum-containing liquid waste for GPSR samples with and without sand.

Because no significant differences were observed in the compressive strength results of the samples cured for 5, 6, 7, and 8 days, a curing time of 7 days was selected for the monoliths prepared henceforth.

3.3 Effect of simulated liquid waste incorporation on the synthesis of geopolymers

3.3.1 Metakaolin SR

Figure 4 shows the compressive strength of geopolymers prepared from SR kaolin, with (GPSR-S) and without sand (GPSR), and a 10 M NaOH–sodium silicate activating solution, incorporating varying mass fractions of simulated aluminum-containing liquid waste. The samples were cured at 60 °C for 7 days.

As shown in Figure 4, increasing the proportion of simulated liquid waste generally reduces the compressive strength, with samples prepared without sand exhibiting higher strength than those containing sand. This behavior is likely due to an increase in the material porosity caused by the excess water in the mixture, resulting from the higher incorporation of simulated aluminum-containing liquids. It has been reported that mechanical strength decreases with increasing molar water content, as higher water content leads to greater porosity and consequently lower compressive strength (Kuenzel et al., 2014). In addition, a higher amount of liquid in the mixture reduces the NaOH concentration available to dissolve metakaolin particles, thereby limiting the formation of soluble aluminosilicate species required to polymerize with the silicate chains from the activating solution and form the geopolymer network (Wang et al., 2005; Cong and Cheng, 2021).

The results indicate that at low liquid content (10%), the compressive strength is very low, whereas the highest strength values were obtained at 20% liquid content for both sand-containing and sand-free samples. It is likely that at both low and very high aluminum concentrations within the mixture, secondary reactions occur that reduce the amount of reactive aluminum available for geopolymer formation. It has been reported that, under highly alkaline conditions, aluminum can react with sand particles to passivate their surfaces, thereby decreasing their solubility in the activating solution and reducing the amount of aluminum available for geopolymer formation (Hay and Ostertag, 2019). An acceptable compressive strength development was obtained at 20% liquid addition; however, it remained lower than that of the pure geopolymer without added liquid (GPSR-0, with and without sand).

Figure 5 shows the XRD patterns of the geopolymers without sand (GPSR-X) obtained by varying the aluminum-containing liquid content at mass fractions of 10, 20, 30, and 40%. Geopolymers with sand (GPSR-XS) are shown in SI (Supplementary Figure SI2). It can be observed that, for both the geopolymers without and with sand, the broad metakaolin band

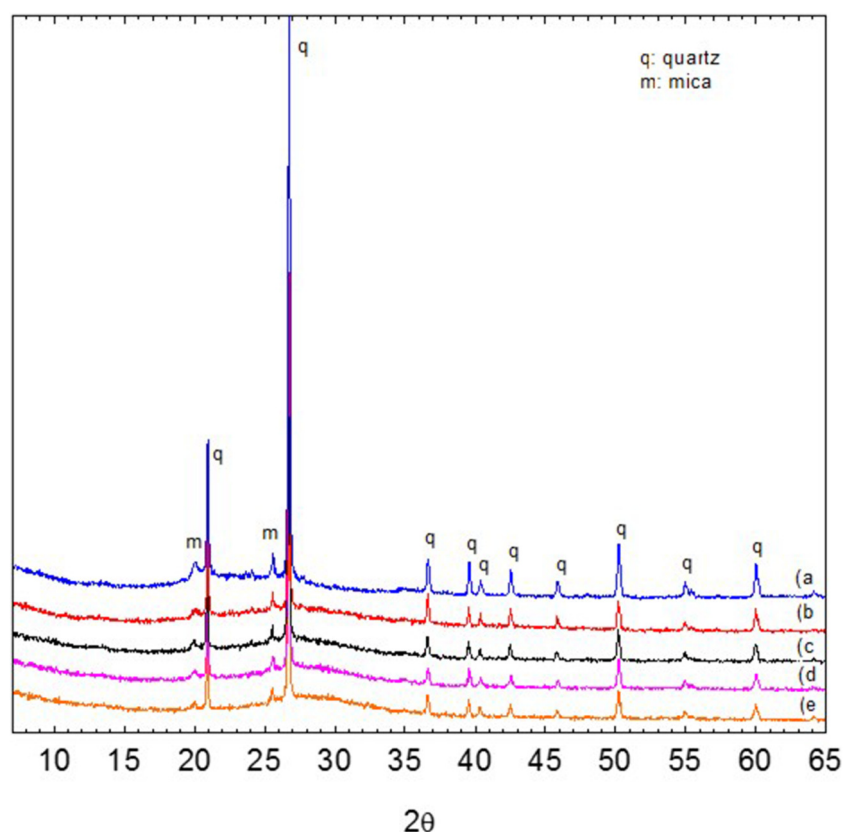


FIGURE 5
XRD patterns of GPSR-X: (a) MKSR, (b) GPSR-10, (c) GPSR-20, (d) GPSR-30, and (e) GPSR-40.

between 18° and 25° shifts toward 25° – 35° , a change characteristic of aluminosilicate gel formation (Zhang et al., 2012). The intensity of this broad band increases slightly with higher liquid content in both GPSR-X and GPSR-XS samples, while no significant changes are observed in the quartz peaks.

Regarding the surface morphological analysis, the SEM micrographs (Figure 6) reveal noticeable changes in the microstructure of the materials, both for samples synthesized with and without sand. The samples containing 10% simulated liquid waste (GPSR-10S, Figure 6a, and GPSR-10; Figure 6d) exhibit a morphology very similar to that of the precursor metakaolin MKSR (Figure 3a), characterized by solid flake-like particles. As the liquid content increases, the samples display higher apparent porosity and a reduction in the amount of solid MKSR particles, which is more evident in the samples prepared with 30% simulated liquid content without sand (GPSR-30, Figure 6f). The high presence of MKSR particles in samples with 10% liquid content (Figures 6a,d) and the pronounced porosity in those prepared with 30% liquid content (Figures 6c,f) suggest poor aluminosilicate gel development, resulting in low compressive strength. Conversely, an intermediate degree of porosity and MKSR particle size (Figures 6b,e) appears to be associated with an acceptable development of the mechanical properties of the materials.

Under the evaluated experimental conditions, a 20% addition of simulated liquid waste can be considered the optimal level for

producing MKSR-based geopolymers with acceptable compressive strength.

3.3.2 Metakaolin S

Figure 7 shows the compressive strength of MKS-based geopolymers prepared with and without sand, incorporating 10, 20, and 30% simulated liquid waste. Samples GPS-0 and GPS-0S correspond to geopolymers without simulated liquid addition. The samples containing 40% simulated liquid (GPS-40 and GPS-40S) waste broke during demolding; therefore, its compressive strength could not be measured.

MKS-based geopolymers show a consistent decrease in compressive strength with increasing simulated liquid content, the effect being more pronounced in sand-free samples, except for the one containing 30% liquid. This behavior is likely related to the previously discussed effect of increased water content, which on one hand enhances the porosity of the samples, making them less resistant to compression, and on the other hand reduces the concentration of the sodium silicate–NaOH activating solution. This reduction limits the dissolution of metakaolin particles and consequently decreases the formation and availability of aluminosilicate species involved in geopolymer formation (Wang et al., 2005; Kuenzel et al., 2014; Cong and Cheng, 2021).

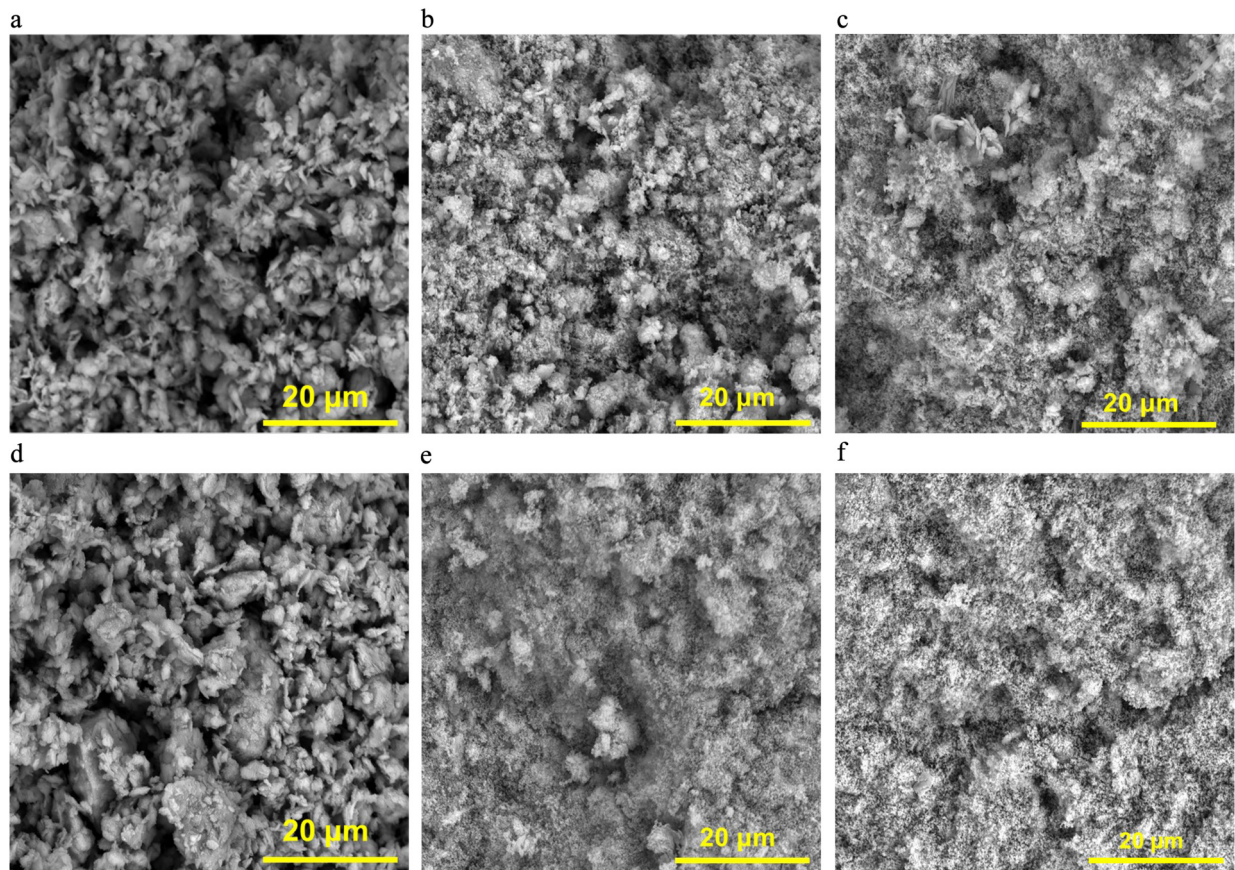


FIGURE 6 Micrographs of GP samples: (a) GPSR-10S, (b) GPSR-20S, (c) GPSR-30S, (d) GPSR-10, (e) GPSR-20, and (f) GPSR-30.

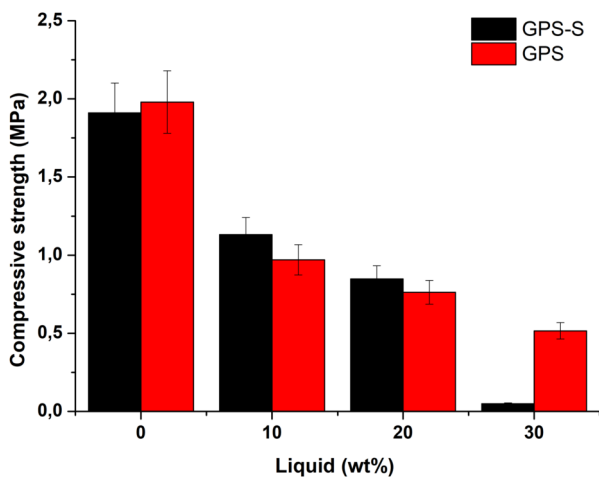


FIGURE 7 Compressive strength versus mass percent of simulated aluminum-containing liquid waste for GPS samples with and without sand.

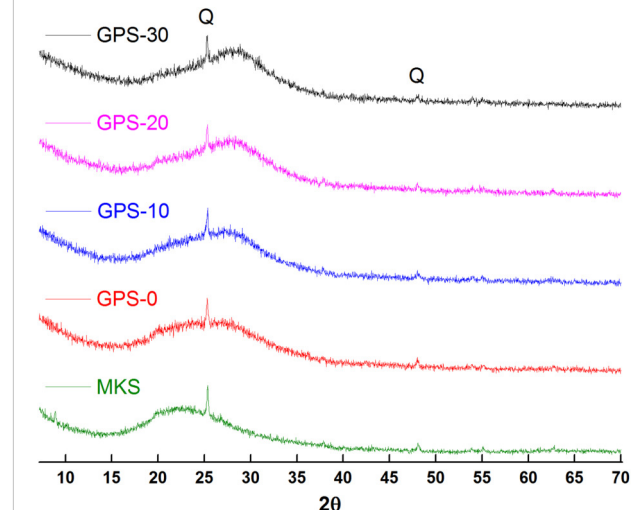


FIGURE 8 XRD patterns of GPS-X.

The presence of sand appears to slightly improve compressive strength. It is possible that aluminum passivation reactions are reduced in this case. However, all samples exhibit low compressive strength, indicating that the evaluated conditions are suboptimal for aluminosilicate gel formation with MKS. The GPS-30S sample showed very low strength, likely due to incomplete setting resulting from the high simulated liquid content.

XRD patterns of sand-free samples (GPS-X, Figure 8) reveal a shift of the MKS band from 15°–25° to 25°–35°, characteristic of geopolymer formation (Cong and Cheng, 2021). The band intensity increases slightly with higher liquid content, while quartz peaks remain largely unchanged. All MKS-based sand-free geopolymers are predominantly amorphous. On the other hand, sand-containing samples (see SI, Supplementary Figure SI3) display quartz peaks from the sand, which remain largely unchanged with increasing liquid content. The MKS broad band shifts slightly from 15°–25° to 25°–35°, though the change is barely noticeable. Sand may enhance structural integrity by reducing porosity, but this is insufficient to significantly improve compressive strength.

SEM micrographs for GPS (see SI, Supplementary Figure SI4) show no significant differences between geopolymers without added liquid and those with simulated liquid waste. Solid MKS particles are present in all samples, suggesting incomplete metakaolin dissolution in the sodium silicate-NaOH solution and hence, insufficient geopolymer development.

Under the tested conditions, MKS-based geopolymers containing simulated liquid waste did not achieve acceptable compressive strength. Further optimization will be addressed in future studies.

4 Conclusion

Metakaolin-based geopolymers were successfully synthesized from two kaolin sources (SR and S) and evaluated for their potential use in the immobilization of simulated aluminum-containing liquid radioactive waste. Calcination at 800 °C was sufficient to obtain reactive metakaolin suitable for geopolymer formation.

The curing time had an effect on the mechanical properties of the materials, with compressive strength increasing up to 6 days of curing at 60 °C, after which no further improvement was observed. The incorporation of simulated liquid waste influenced the mechanical and structural characteristics of the geopolymers. Increasing liquid content generally reduced compressive strength due to increased porosity and reduced metakaolin dissolution in the alkaline activator.

For geopolymers based on SR metakaolin, the optimal performance was obtained at 20 wt% simulated liquid waste addition, which produced an aluminosilicate matrix with acceptable compressive strength. In contrast, geopolymers prepared from S metakaolin exhibited lower strength and incomplete geopolymerization under the same conditions, indicating that the Si/Al ratio and precursor composition strongly affect the reactivity and structure of the final product.

Overall, SR-based geopolymers demonstrated promising properties for use as solid matrices in the stabilization and immobilization of aluminum-bearing radioactive liquid waste. Future work should focus on optimizing formulation parameters, investigating long-term durability, and evaluating radionuclide retention and leaching behavior to confirm their suitability for nuclear waste management applications.

Data availability statement

The raw data supporting the conclusions of this article will be made available by the authors, without undue reservation.

Author contributions

WT: Investigation, Data curation, Project administration, Validation, Conceptualization, Supervision, Writing – review and editing, Resources, Methodology, Writing – original draft, Formal Analysis, Software, Visualization. AT: Methodology, Investigation, Formal Analysis, Software, Data curation, Writing – original draft. LD: Formal Analysis, Investigation, Writing – original draft, Data curation, Methodology. DA: Data curation, Writing – original draft, Formal Analysis. AM: Funding acquisition, Writing – review and editing, Writing – original draft, Conceptualization, Resources, Validation, Investigation, Project administration, Formal Analysis, Supervision, Data curation, Software, Methodology.

Funding

The author(s) declared that financial support was received for this work and/or its publication. The authors would like to thank Natalia Grattone and Nicolás Taboada from DITA for their support and collaboration, as well as Frontiers for funding the publication cost. As this work is part of the R&D activities within the Department, the equipment and materials were provided by our Management, PNGRR (CNEA).

Conflict of interest

The author(s) declared that this work was conducted in the absence of any commercial or financial relationships that could be construed as a potential conflict of interest.

Generative AI statement

The author(s) declared that generative AI was used in the creation of this manuscript. For technical translation, from spanish to english.

Any alternative text (alt text) provided alongside figures in this article has been generated by Frontiers with the support of artificial intelligence and reasonable efforts have been made to ensure

accuracy, including review by the authors wherever possible. If you identify any issues, please contact us.

Publisher's note

All claims expressed in this article are solely those of the authors and do not necessarily represent those of their affiliated organizations, or those of the publisher, the editors and the reviewers. Any product

that may be evaluated in this article, or claim that may be made by its manufacturer, is not guaranteed or endorsed by the publisher.

Supplementary material

The Supplementary Material for this article can be found online at: <https://www.frontiersin.org/articles/10.3389/fnuen.2025.1738676/full#supplementary-material>

References

- Arbel-Haddad, M., Harnik, Y., Schlosser, Y., and Goldbourt, A. (2022). Cesium immobilization in metakaolin-based geopolymers elucidated by ^{133}Cs solid state NMR spectroscopy. *J. Nucl. Mater.* 562, 153570. doi:10.1016/j.jnucmat.2022.153570
- Barbosa, V. F. F., Mackenzie, K. J. D., and Thaumaturgo, C. (2000). Synthesis and characterisation of materials based on inorganic polymers of alumina and silica: sodium polysialate polymers. *Int. J. Inorg. Mater.* 2, 309–317. doi:10.1016/s1466-6049(00)00041-6
- Cong, P., and Cheng, Y. (2021). Advances in geopolymer materials: a comprehensive review. *J. Traffic Transp. Eng. Engl. Ed.* 8 (3), 283–314. doi:10.1016/j.jtte.2021.03.004
- Davidovits, J. (2020). *Geopolymer: chemistry and applications*. 5th ed. Saint-Quentin, France: Institut Géopolymère.
- Duxson, P., Provis, J. L., Lukey, G. C., Mallicoat, S. W., Kriven, W. M., and van Deventer, J. S. (2005). Understanding the relationship between geopolymer composition, microstructure and mechanical properties. *Colloids Surf. A Physicochem Eng. Asp.* 269 (1–3), 47–58. doi:10.1016/j.colsurfa.2005.06.060
- Duxson, P., Mallicoat, S. W., Lukey, G. C., Kriven, W., and van Deventer, J. (2007). The effect of alkali and Si/Al ratio on the development of mechanical properties of metakaolin-based geopolymers. *Colloids Surf. A Physicochem Eng. Asp.* 292 (1), 8–20. doi:10.1016/j.colsurfa.2006.05.044
- El Alouani, M., Saufi, H., Moutaoukil, G., Alehyen, S., Nematollahi, B., Belmaghraoui, W., et al. (2021). Application of geopolymers for treatment of water contaminated with organic and inorganic pollutants: state-Of-the-art review. *J. Environ. Chem. Eng.* 9, 105095. doi:10.1016/j.jece.2021.105095
- Elmibi, A., Tchakoute, H. K., and Njopwouo, D. (2011). Effects of calcination temperature of kaolinite clays on the properties of geopolymer cements. *Constr. Build. Mater* 25 (6), 2805–2812. doi:10.1016/j.conbuildmat.2010.12.055
- Garces, J. I. T., Tigue, A. A. S., and Promentilla, M. A. B. (2022). A systematic mapping Study of geopolymers for radioactive waste management. *Chem. Eng. Trans.* 94, 1345–1350. doi:10.3303/CET2294224
- García-Mejía, T. A., and de Lourdes Chávez-García, Ma (2016). Compressive strength of Metakaolin-Based geopolymers: influence of KOH concentration, temperature, time and relative humidity. *Mater. Sci. Appl.* 07 (11), 772–791. doi:10.4236/msa.2016.711060
- Geddes, D. A., Walkley, B., Galliard, C. Le, Hayes, M., Bernal, S. A., and Provis, J. L. (2024). Effect of exposure of metakaolin-based geopolymer cements to gamma radiation. *J. Am. Ceram. Soc.* 107 (7), 4621–4630. doi:10.1111/jace.19747
- Glukhovskiy, D. (1959). *Soil silicates*. Kiev: Gosstroyzdat USSR.
- Hay, R., and Ostertag, C. P. (2019). On utilization and mechanisms of waste aluminium in mitigating alkali-silica reaction (ASR) in concrete. *J. Clean. Prod.* 212, 864–879. doi:10.1016/j.jclepro.2018.11.288
- International Atomic Energy Agency (2013). *The behaviours of cementitious materials in long term storage and disposal of radioactive waste: results of a coordinated research project*. International Atomic Energy Agency.
- Internationale Atomenergie-Organisation (2003). *Radioactive waste management glossary*. Vienna, Austria: IAEA.
- Jang, J. G., Park, S. M., and Lee, H. K. (2016). Physical barrier effect of geopolymeric waste form on diffusivity of cesium and strontium. *J. Hazard Mater* 318, 339–346. doi:10.1016/j.jhazmat.2016.07.003
- Khalil, M. Y., and Merz, E. (1994). Immobilization of intermediate-level wastes in geopolymers. *J. Nucl. Mater.* 211, 141–148. doi:10.1016/0022-3115(94)90364-6
- Kuenzel, C., Li, L., Vandeperre, L., Boccaccini, A., and Cheeseman, C. (2014). Influence of sand on the mechanical properties of metakaolin geopolymers. *Constr. Build. Mater* 66, 442–446. doi:10.1016/j.conbuildmat.2014.05.058
- Li, Q., Sun, Z., Tao, D., Xu, Y., Li, P., Cui, H., et al. (2013). Immobilization of simulated radionuclide $^{133}\text{Cs}^+$ by fly ash-based geopolymer. *J. Hazard Mater.* 262, 325–331. doi:10.1016/j.jhazmat.2013.08.049
- Marabini, S. G. (2023). *Inmovilización de residuos radiactivos con cemento portland*. [Buenos Aires]. Buenos Aires, Argentina: Universidad Nacional de San Martín.
- Munthali, M. W., Johan, E., Aono, H., and Matsue, N. (2015). Cs + and Sr 2+ adsorption selectivity of zeolites in relation to radioactive decontamination. *J. Asian Ceram. Soc.* 3 (3), 245–250. doi:10.1016/j.jascer.2015.04.002
- Palomo, A., Grutzeck, M. W., and Blanco, M. T. (1999). Alkali-activated fly ashes. A cement for the future. *Cem. Concr. Res.* 29, 1323–1329. doi:10.1016/s0008-8846(98)00243-9
- Pao, K. S. J. H., and Chin, J. (2022). Effect of additives on immobilization of Se(VI) and Cr(VI) in geopolymer. *Ceram. Soc.* 50, 46–1335.
- Perera, D., Vance, E., Kiyama, S., Aly, Z., and Yee, P. (2007). Geopolymers as candidates for the immobilisation of low-and intermediate-level waste. *Mater. Res. Soc. Symp. Proc.* 985. doi:10.1557/proc-985-0985-nn10-01
- Phair, J. W., and Van Deventer, J. S. J. (2002). Effect of the silicate activator pH on the microstructural characteristics of waste-based geopolymers. *Int. J. Min. Process.* 66, 121–143. doi:10.1016/s0301-7516(02)00013-3
- Rovnanik, P. (2010). Effect of curing temperature on the development of hard structure of metakaolin-based geopolymer. *Constr. Build. Mater* 24 (7), 1176–1183. doi:10.1016/j.conbuildmat.2009.12.023
- Stevenson, M., Place, B., and Adelaide, N. (2005). Relationships between composition, structure and strength of inorganic polymers part 2 fly ash-derived inorganic polymers. *J. Mater. Sci.* 40, 4247–4259. doi:10.1007/s10853-005-1226-2
- Tian, Q., Nakama, S., and Sasaki, K. (2019). Immobilization of cesium in fly ash-silica fume based geopolymers with different Si/Al molar ratios. *Sci. Total Environ.* 687, 1127–1137. doi:10.1016/j.scitotenv.2019.06.095
- Tri, P. Q., Maes, N., and Zlobenko, B. (2021). *Proceedings PREDIS may workshop 2021 immobilization of the treated wastes by geopolymer or cement-based materials encapsulated or by molten glass coating*, 72–76.
- Wang, H., Li, H., and Yan, F. (2005). Synthesis and mechanical properties of metakaolinite-based geopolymer. *Colloids Surf. A Physicochem Eng. Asp.* 268 (1–3), 1–6. doi:10.1016/j.colsurfa.2005.01.016
- Wang, Y., Han, F., and Mu, J. (2018). Solidification/Stabilization mechanism of Pb(II), Cd(II), Mn(II) and Cr(III) in fly ash based geopolymers. *Constr. Build. Mater* 160, 818–827. doi:10.1016/j.conbuildmat.2017.12.006
- Zhang, Z., Wang, H., Provis, J. L., Bullen, F., Reid, A., and Zhu, Y. (2012). Quantitative kinetic and structural analysis of geopolymers. Part 1. the activation of metakaolin with sodium hydroxide. *Thermochim. Acta* 539, 23–33. doi:10.1016/j.tca.2012.03.021
- Zhang, H. Y., Kodur, V., Cao, L., and Qi, S. I. (2014). Fiber reinforced geopolymers for fire resistance applications. *Procedia Eng.* 71, 153–158. doi:10.1016/j.proeng.2014.04.022
- Zhang, Z. H., Zhu, H. J., Zhou, C. H., and Wang, H. (2016). Geopolymer from kaolin in China: an overview. *Appl. Clay Sci.* 119, 31–41. doi:10.1016/j.clay.2015.04.023
- Zheng, Z., Li, Y., Zhang, Z., and Ma, X. (2020). The impacts of sodium nitrate on hydration and microstructure of Portland cement and the leaching behavior of Sr²⁺. *J. Hazard Mater* 388, 121805. doi:10.1016/j.jhazmat.2019.121805